The Attentional Blink Impairs Detection and Delays Encoding of Visual Information: Evidence from Human Electrophysiology

Roberto Dell'Acqua[1], Paul E. Dux[2], Brad Wyble[3], Mattia Doro[1],
Paola Sessa[1], Federica Meconi[1], and Pierre Jolicœur[4]

Abstract

■ This article explores the time course of the functional interplay between detection and encoding stages of information processing in the brain and the role they play in conscious visual perception. We employed a multitarget rapid serial visual presentation (RSVP) approach and examined the electrophysiological P3 component elicited by a target terminating an RSVP sequence. Target-locked P3 activity was detected both at frontal and parietal recording sites and an independent component analysis confirmed the presence of two distinct P3 components. The posterior P3b varied with intertarget lag, with diminished amplitude and postponed latency at short relative to long lags—

an electroencephalographic signature of the attentional blink (AB). Under analogous conditions, the anterior P3a was also reduced in amplitude but did not vary in latency. Collectively, the results provide an electrophysiological record of the interaction between frontal and posterior components linked to detection (P3a) and encoding (P3b) of visual information. Our findings suggest that, although the AB delays target encoding into working memory, it does not slow down detection of a target but instead reduces the efficacy of this process. A functional characterization of P3a in attentive tasks is discussed with reference to current models of the AB phenomenon. ■

INTRODUCTION

One of the most enduring issues in cognitive neuroscience concerns the neural substrate(s) underling conscious perception. This has been a topic of intense investigation for several decades, and despite a definitive understanding of the neural underpinnings of consciousness remaining elusive, there is a general consensus that conscious perception is not tied to a single neural structure but rather reflects the interplay of distinct brain areas. For example, Dehaene, Sergent, and Changeux (2003) and Baars (1989) hypothesize that conscious perception represents the engagement of a global neural workspace. Specifically, for a stimulus to enter consciousness, neurons with long-distance axons that are capable of connecting distinct brain regions must be activated, which then allows communication between higher-level processing areas and those that are involved in sensory analysis. Similarly, Lamme and colleagues (Fahrenfort, Scholte, & Lamme, 2007; Lamme & Roelfsema, 2000) and Di Lollo, Enns, and Rensink (2000) predict that for information to be accessed consciously not only must it pass from sensory to higher-level structures but must also be fed back, and it is through these reentrant iterations that conscious representations are established.

A key phenomenon for studying conscious perception is the attentional blink (AB) (Raymond, Shapiro, & Arnell, 1992)—participants' typically impaired ability to perceive the second of two targets (T2) in a rapid serial visual presentation (RSVP) if it appears within 200–500 msec of a first target (T1). Paradoxically, T2 is much easier to report when it follows T1 immediately. This effect is referred to as *lag 1 sparing* and it is thought to reflect T1 and T2 being processed together within a single attentional episode (Dell'Acqua, Dux, Wyble, & Jolicœur, 2012; Wyble, Potter, Bowman, & Nieuwenstein, 2011; Wyble, Bowman, & Nieuwenstein, 2009; Chun & Potter, 1995). fMRI (Choi, Chang, Shibata, Sasaki, & Watanabe, 2012; Kranczioch, Debener, Schwarzbach, Goebel, & Engel, 2005; Marois & Ivanoff, 2005; Marois, Yi, & Chun, 2004; Marcantoni, Lepage, Beaudoin, Bourgouin, & Richer, 2003) and PET (Slagter et al., 2012) explorations have localized AB effects to a frontoparietal network composed of core nodes in the posterior parietal and dorsolateral pFC that support a variety of attention tasks (e.g., Corbetta & Shulman, 2002; Desimone & Duncan, 1995). A set of additional areas have been shown to be susceptible to the AB influence, including striate (Williams, Visser, Cunnington, & Mattingley, 2008) and extrastriate visual areas (e.g., Dell'Acqua, Sessa, Jolicœur, & Robitaille, 2006; Marois et al., 2004), and subcortical structures (i.e., BG and locus coeruleus), whose roles have been incorporated in neural instantiations of

[1]University of Padova, [2]The University of Queensland, [3]Pennsylvania State University, [4]Université de Montréal

AB models (Colzato, Slagter, de Rover, & Hommel, 2011; Hommel et al., 2006; Nieuwenhuis, Gilzenrat, Holmes, & Cohen, 2005).

Evidence converging with the hypothesis that the AB engages a frontoparietal attention circuit comes from studies employing EEG and MEG techniques that have explored the correspondence between AB effects and non-phase-locked (Bastiaansen, Mazaheri, & Jensen, 2012) neural synchronization of scalp-recorded oscillations. AB-induced decreases in long-range phase synchronization in the beta and gamma band encompassing the frontoparietal attention network have been reported by Kranczioch, Debener, Maye, and Engel (2007), Nakatani, Ito, Nikolaev, Gong, and van Leeuwen (2005), and Gross et al. (2004). These modulations were consistently observed before T1 onset, a pattern akin to spontaneous trial-by-trial fluctuations in alpha band (de)synchronization which has been proposed to index an anticipatory mental state related to successful identification of RSVP targets (MacLean & Arnell, 2011; see Hanslmayr, Gross, Klimesch, & Shapiro, 2011, for a review). However, although these studies have helped isolate processing to specific attentional circuits within the brain, it is not known how these circuits interact to produce the AB. For example, it could be the case that the AB slows down the detection of T2, allowing it to be overwritten by trailing stimuli. On the other hand, it could be that T2 detection operates unimpaired, but that the ensuing attentional deployment is less effective at processing the required information.

A key approach for isolating the stages of information processing that gives rise to the AB is the ERP technique. Studies employing this approach have focused primarily on AB modulations of the P3b component. Typically observed at midparietal electrode sites, this waveform has been shown to reflect consolidation of visual information in short-term/working memory (Akyürek, Leszczyński, & Schubö, 2010). Indeed, P3b can be taken as the hallmark of a widespread state of activation following detection of visual target information aiding memory encoding (Kranczioch, Debener, & Engel, 2003; Fabiani & Donchin, 1995; Johnson, 1995). Two complementary studies have demonstrated that the AB must reflect, at least to some extent, T2 memory consolidation being postponed when the two targets appear in close temporal proximity in an RSVP stream. By using standard RSVP trials terminating with one or more distractors following T2, Vogel, Luck, and Shapiro (1998) showed that T2-locked P3b is influenced by the AB, in the form of a sizable T2-locked P3b amplitude reduction at short relative to long lags. T2-locked ERP components preceding P3b on the temporal scale (e.g., P1, N1, N170, and N400) were found to be unaffected by the AB perturbation (for converging evidence, see also Harris, McMahon, & Woldorff, 2013; Batterink, Karns, Yamada, & Neville, 2010). Using a modified version of this RSVP design, Sessa, Luria, Verleger, and Dell'Acqua (2007) displayed RSVP trials terminated by an unmasked T2 (i.e., T2 was not followed by distractors) and found a T2-locked P3b latency postponement at short relative to long T1–T2 lags (for similar results, see also Brisson & Bourassa, 2014; Ptito, Arnell, Jolicœur, & MacLeod, 2008). Note that the behavioral correlate of the AB (i.e., a reduction of T2 report at short T1–T2 lags) was significantly attenuated under these conditions, as the unmasked T2 could persist within sensory and information memory systems (Coltheart, 1980) and thereby outlast the attentional impairment (e.g., Giesbrecht & Di Lollo, 1998). Another study of the P3b recording indicated that it has increased variability during the AB, which is consistent with the aforementioned findings, and suggests that the amount of delay in T2 processing varies from one trial to the next (Chennu, Craston, Wyble, & Bowman, 2009). Interestingly, the finding of delayed processing in posterior areas during the AB was extended by Scalf, Dux, and Marois (2011), who employed time-resolved fMRI to find delayed activation of occipital areas for T2 displayed during the AB. The neural sources of the P3b have been localized to posterior brain structures including posterior-parietal areas and the TPJ (e.g., Polich, 2003; Johnson, 1993).

The above AB and P3b findings fit well with behavioral studies, which suggest that T2 processing is delayed during the AB, which renders it more vulnerable to interruption from subsequent stimuli. However, what cannot be determined from these measurements of the P3b is whether it is the detection or the additional encoding of T2 that is delayed. To address this question, we consider a different component associated with the detection of relevant stimuli, namely, P3a. P3a is typically observed at midfrontal electrodes and occurs before the P3b. Lesion studies (Knight, 1991), fMRI/EEG multimodal acquisition (Bledowski, Prvulovic, Goebel, Zanella, & Linden, 2004; Bledowski, Prvulovic, Hoechstetter, et al., 2004), and neurobiological analyses (Gazzaniga, Ivry, & Mangun, 2000) have pointed to a set of frontal structures generating P3a that include anterior cingulate and lateral prefrontal cortices (Friedman, Cycowicz, & Gaeta, 2001). Whereas earlier proposals have suggested that the P3a primarily indicates novelty and sensory deviance of cross-modal stimulation (e.g., Courchesne, Hillyard, & Galambos, 1975), more recent views on P3a link it to the deployment of attention for detection of contextually salient information presented amongst distracting stimuli (e.g., Polich, 2007; Barceló, Escera, Corral, & Periáñez, 2006; Koechlin, Ody, & Kouneiher, 2003; Cycowicz & Friedman, 1998), especially in tasks where such classification is difficult (Polich & Comerchero, 2003).

Using a behavioral approach, we (Dux, Wyble, Jolicœur, & Dell'Acqua, 2014) recently examined whether the AB delays target detection, memory encoding or both, and whether the AB is a T1-locked phenomenon or a manifestation of an attentional perturbation induced by distracting information trailing T1 (see Martens & Wyble, 2010; Dux & Marois, 2009, for reviews about these differing

theoretical positions). Specifically, we assessed if the encoding load within a temporal attention episode/window influenced report of stimuli appearing in subsequent episodes. In a three-target RSVP paradigm, T1 and T2 always appeared sequentially, creating lag 1 sparing conditions, but T3 appeared at varying lags relative to T2. When T1 and T2 were correctly reported a much larger AB was observed for T3 compared with when only T1 or T2 was correctly reported. Thus, target load, within an attentional window and independent of distractors, influenced the AB magnitude. In addition, there was no difference between the AB observed when either T1 or T2 was missed in three-target trials relative to the AB found in standard two-target trials, suggesting the missing one stimulus preceding T3 had an all-or-none effect on the AB observed in three-target trials.

Here, we combine the approach of Dux et al. (2014) with ERPs to investigate the influence of target load on the interplay between detection and encoding stages and the role they play in operations linked to the AB and conscious visual perception. Specifically, we use a variant of the three-target RSVP paradigm introduced by Dux et al. (2014) to explore the impact target processing load has on P3a and P3b components elicited by the last target in RSVP streams. The design differs from that employed by Dux et al. (2014) in two important aspects. First, the last target embedded in RSVP was not trailed by distractors so as to allow us to observe fully fledged P3b and P3a responses to this stimulus. Little or no behavioral AB is typically observed for unmasked targets (e.g., Jannati, Spalek, Lagroix, & Di Lollo, 2012; Jannati, Spalek, & Di Lollo, 2011; Ptito et al., 2008; Sessa et al., 2007; Giesbrecht & Di Lollo, 1998). However, under these conditions, the underlying neural process evoked by T1 that produces the behavioral AB for a masked T2 should still occur, and it is this underlying neural process that is the subject of our inquiry. This approach has the benefit of allowing us to capture the modulatory influence of our manipulations on the neural correlates of target processing as quantifiable parametric changes in the latency and amplitude of the P3a/b components. Second, target-present trials in the conditions of interest were intermixed in the present experimental context with target-absent trials (i.e., trials in which the last target was replaced with a distractor), so as to isolate unequivocal P3a/b responses reflecting last target detection and encoding uncontaminated by activity elicited by to-be-ignored distractors and/ or by phasic oscillations induced by the RSVP rhythm (Hanslmayr et al., 2011; Ptito et al., 2008).

METHODS

Participants

Forty students at the University of Padua (23 women) participated in the experiment after giving informed consent. Their mean age was 24.8 years (*SD* = 4.6 years), and all had normal or corrected-to-normal visual acuity and no history of neurological disorders.

Stimuli

The stimuli were the 22 letters of the English alphabet remaining after excluding B, I, O, Z, and the digits 2–9. The stimuli were displayed in light gray (34 cd/m^2) Romantri font against a black (6 cd/m^2) background. Luminance measurements were performed using a Minolta LS-100 chroma-meter (Ramsey, NJ). Stimuli appeared on a 19-in. CRT monitor running at 60 Hz, placed at a viewing distance of approximately 60 cm from the participant, controlled by an i686 IBM-clone computer running MEL 2.0 software. RSVP streams were composed of distractor digits randomly selected from the available set, plus two or three different target letters (T1, T2, and T3) presented in various positions in the stream (see Design and Procedure section). Identical distractor digits in the RSVP stream were always separated by a minimum of three different stimuli. Each stimulus was displayed for 84 msec and was immediately replaced by the next stimulus (ISI = 0 msec). The lag between pairs of critical targets (i.e., T1–T2 lag in the two-target RSVP streams or T2–T3 lag in three-target RSVP streams) was manipulated by varying the number of distractors between T1 and T2 or between T2 and T3. The number of distractors preceding T1 was varied randomly across trials from 6 to 11, and each RSVP stream ended with T2 in two-target RSVP streams or T3 in three-target RSVP stream, which were replaced by a digit distractor in the same position when the last target was not displayed. All stimuli were scaled to fit in a central, square portion of the monitor measuring 1.0° × 1.0° of visual angle.

Design and Procedure

A schematic representation of the experimental design is illustrated in the upper portion of Figure 1. In three-target RSVP streams, T1 and T2 were always consecutive items. The lag between T1 and T2 in two-target RSVP streams and between T2 and T3 in three-target RSVP streams was manipulated by presenting 2 (lag 3, SOA = 252 msec) or 8 (lag 9, SOA = 756 msec) distractors between these targets.

Each participant performed 648 trials, organized into 18 blocks of 36 trials each. Each lag appeared an equal number of times in each block, but their order was pseudo-randomized, with the constraint that no more than three consecutive trials could be displayed at the same lag. The last target in two-target (i.e., T2) and three-target (i.e., T3) RSVP streams was displayed on half of the trials (henceforth, target-present trials) within each block and replaced with a digit distractor in the same position on the other half of trials (henceforth, target-absent trials). In four trials in each block, a target was presented in the last stream position, with no preceding targets. These trials were

not analyzed in this study. Half of the participants started with nine consecutive blocks of two-target RSVP streams, followed by nine consecutive blocks of three-target RSVP streams. The opposite order applied for the other half of the participants.

Each trial began with the presentation of a number of horizontally aligned plus signs in the center of the monitor denoting the number of targets that would appear in the forthcoming RSVP stream (i.e., two or three plus signs). Pressing the spacebar initiated a trial, causing the plus signs to disappear, and the RSVP to start 800 msec later. A question was displayed 800 msec after the end of the RSVP stream, inviting report of the targets by pressing the corresponding keys on the keyboard. Participants were instructed to report all letters in the RSVP streams, with no emphasis on their order or response speed. Feedback on an incorrectly reported target was provided at the end of each trial by replacing the plus sign in the position congruent with target order (from left to right, T1, T2, and T3 when present) with a minus sign. Experimental data were collected after exposing participants to no less than 20 RSVP streams for practice in each of two-target and three-target conditions.

EEG/ERP Recordings and Preprocessing

EEG activity was recorded continuously from 32 active electrodes (Fp1, Fp2, Fz, F3, F4, F7, F8, FCz, C3, C4, Cz, CP1, CP2, CP5, CP6, P3, P4, Pz, O1, O2, Oz, T7, T8, TP9, PO9, PO10, P7, P8 sites) placed on an elastic Acti-Cap (Brain Products, München, Germany), referenced to the left earlobe. HEOG activity was recorded bipolarly from electrodes positioned on the outer canthi of both eyes. VEOG activity was recorded bipolarly from two electrodes, above (Fp1) and below the left eye. Impedance at each electrode site was maintained below 5 KΩ. EEG, HEOG, and VEOG activities were amplified, filtered using a band-pass of 0.016–80 Hz, digitized at a sampling rate of 500 Hz, and referenced offline to the average of the left and right earlobes. Independent components analysis (ICA) was used to identify blink and saccade components in the continuous EEG recordings and remove them from the data (Delorme & Makeig, 2004; Jung et al., 2000). The corrected EEG was high-pass filtered at 0.1 Hz and low-pass filtered at 20 Hz and then segmented into 1100 msec epochs starting 100 msec before the onset of the last character in the RSVP stream and ending 1000 msec after and baseline-corrected using the mean activity in the interval [−100, 0] msec. To ensure no residual artifacts
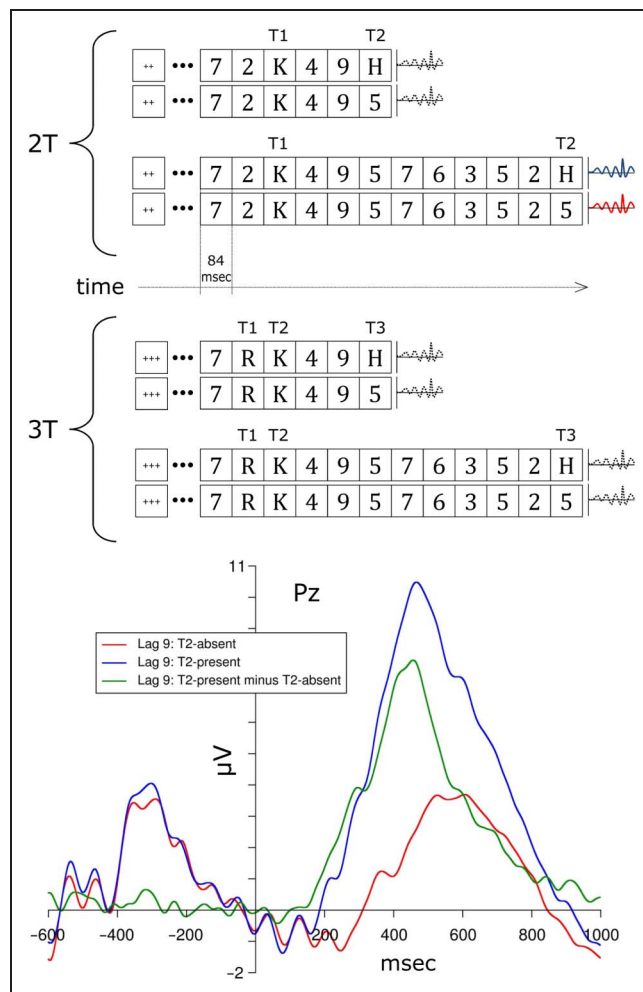

Figure 1. Top: Gantt diagrams: Design of the present experiment. In target-present trials, two letters or three letters were embedded among digit distractors in two-target (2T) or three-target (3T) RSVP streams. Both RSVP streams began with the presentation of a number of centrally displayed "+" signs equal to the number of targets included in the RSVP streams, and each character was displayed for 84 msec, immediately followed by the next character. In half of the trials, the last target letter was replaced with a digit distractor, generating a corresponding target-absent RSVP stream. In three-target RSVP streams, the first and second targets (i.e., T1 and T2) were always consecutive letters. T1 and T2 in two-target RSVP streams and T2 and T3 in three-target RSVP streams were separated by two distractors (i.e., at lag 3) or eight distractors (i.e., at lag 9). When present, the last target in both RSVP streams was never trailed by a digit distractor. The dotted curvilinear function trailing the last character in each RSVP stream indicates (the onset of) the target monitored for ERP responses in the present experiment. Bottom graph: Illustration of the subtraction approach used in the present context to isolate difference ERPs reflecting mental operations engaged for last target processing. In the graph, T2-locked ERP functions observed at Pz in two-target trials, at lag 9, in the T2-present (blue) and T2-absent (red) conditions. Corresponding colors can be seen in the Gantt diagrams above referred to the condition of interest. T1-locked P3 responses of equal amplitude peaking at about −300 msec before T2 precede T2-locked P3 responses elicited in target-present (red) and target-absent (blue) trials. P3 responses to the last distractor in target-absent trials were non-nil, had a later onset latency, and were generally of smaller amplitude than P3 responses observed in T2-present trials. Note also that both T2-present and T2-absent trial ERPs show clear symptoms of stimulus-locked visual evoked potentials in the form of entrained sinusoidal activity at about 12 Hz, corresponding to the rate of RSVP stimulation. To derive "pure" target-related ERP activity, target-absent ERP responses were subtracted from target-present ERP responses in each condition of the experimental design (see text). The resulting difference ERP function is shown in green in the graph.

remained on the EOG channels, each segment was examined in the interval $[-100, 1000]$ msec relative to the onset of the last item in the RSVP stream for voltage deviations greater than 80 µV in any period of 150 msec for the VEOG difference waveform or a deviation greater than 45 µV in any 300 msec period for the HEOG difference waveform. Segments with residual ocular artifacts were removed from the data set. EEG channels were flagged when the signal exceeded ±100 µV anywhere in the analysis segment. If a segment had seven or fewer flagged data channels, these channels were interpolated using a spherical spline interpolation algorithm in EEGLAB (Delorme & Makeig, 2004), for that segment. The critical analyses were carried out on separate ERP waveforms for each condition (two-target vs. three-target and lag 3 vs. lag 9) considering only trials associated with the correct report of all displayed targets and generated by subtracting the ERP waveforms elicited by distractors replacing T2 in two-target (target-absent) trials or T3 in three-target (target-absent) trials from the ERP waveforms elicited by the corresponding target-present trials (i.e., T2 in two-target trials or T3 in three-target trials). These difference waveforms isolate the response to a target character in the final RSVP position—T2 or T3, in two-target and three-target trials, respectively—from the response to a nontarget character in the same position while reducing to nil EEG oscillations in phase with the rate of presentation of RSVP items (about 12 Hz; alpha band). An illustration of the results of the present subtractive approach is reported in the lower portion of Figure 1.

The mean amplitude of the subtracted P3a and P3b components was quantified as the mean value in a 150-msec window centered on the peak of the waveform in individual grand averages computed at Fz and Pz, respectively. As noted above, these electrodes have previously been linked with peak amplitude of the P3a and P3b, respectively (e.g., Polich, 2003). The mean latency of the subtracted P3 components at the same recording sites was estimated using the jackknife approach (Kiesel, Miller, Jolicœur, & Brisson, 2008; Ulrich & Miller, 2001) and deriving individual values with the solution proposed by Smulders (2010; see also Brisson & Jolicœur, 2008). Latency values were calculated as the time-point when individual jackknife waveforms reached 75% of the peak amplitude. The Greenhouse–Geisser correction for nonsphericity was applied when appropriate.

RESULTS

Behavior

Separate ANOVAs were performed on the mean proportion of correct report for each target-contingent of the correct report of preceding targets—as a function RSVP structure (two-target trials vs. three-target trials) and Lag

Table 1. Mean Probability of Correct Report of Each Target Included in Two-target (2T) and Three-target (3T) RSVP Streams as a Function of Lag (T1–T2 Lag in 2T RSVP; T2–T3 Lag in 3T RSVP)

| Target | Trial Type | *Lag* | |
		3	*9*
p(T1)	2T	0.94	0.95
	3T	0.81	0.82
p(T2|T1)	2T	0.95	0.96
	3T	0.94	0.94
p(T3|T1 ^ T2)	3T	0.86	0.96

Values in the table are contingent on the correct report of preceding target(s). Highlighted in gray are the results indicating an AB in 3T trials, namely, a lower probability of correct T3 report at T2–T3 lag 3 relative to T2–T3 lag 9.

(3 vs. 9) as within-subject factors. Only target-present trials were considered in the analyses (see Table 1).

On average, T1 report was superior in two-target trials relative to three-target trials, $F(1, 39) = 256.7$, $\eta_p^2 = .868$, $p < .001$, and this effect was constant across lags, $F < 1$. An ANOVA was carried out to compare T2 report in two-target trials and T3 report in three-target trials, as a function of Lag. There was a main effect of Number of targets, $F(1, 39) = 34.7$, $\eta_p^2 = .466$, $p < .001$, a main effect of Lag, $F(1, 39) = 17.3$, $\eta_p^2 = .307$, $p < .001$, and a significant interaction between these factors, $F(1, 39) = 15.9$, $\eta_p^2 = .290$, $p < .001$. False-discovery rate (Benjamini & Hochberg, 1995) corrected t tests indicated that Lag effects were absent on T2 in two-target trials, $t < 1$, whereas T3 report was worse at lag 3 relative to lag 9 in three-target trials, $t(1, 39) = 18.6$, $p < .001$, that is, a small but reliable AB effect was detected in spite of the absence of a distractor trailing T3. These findings converge with prior studies reporting small but reliable AB effects even when the last target is not masked by trailing distractors (Jannati et al., 2011, 2012; Ptito et al., 2008; Sessa et al., 2007; Giesbrecht & Di Lollo, 1998).

ERPs

The various automated artifact screening procedures resulted in the exclusion of 2.4% of the segments. For most participants, less than 1% of the data were excluded. Three participants had exclusion rates between 18% and 22%. Visual inspection of their ERPs suggested their results were comparable to those of the other participants, and so we included their data in final analyses. Thus, the final sample included all 40 participants tested in the experiment.

P3b

Difference (target-present minus target-absent; see EEG/ ERP Recordings and Preprocessing section) P3 response

waveforms for two-target and three-target trials at each lag are shown in Figure 2 for electrode Pz. Key for this study, the amplitude of P3b responses was largest and largely overlapping at lag 9 for two-target and three-target trials but was delayed and attenuated at lag 3. This target-load effect on P3b was substantially more evident in three-target trials than in two-target trials.

The main analyses were performed at Pz, at the peak of the scalp distribution of the P3b component. At lag 9, the mean amplitudes of the P3b were 7.35 μV in two-target trials and 7.13 μV in three-target trials. At lag 3, the mean amplitudes of the P3b were 5.7 μV in two-target trials and 3.35 μV in three-target trials. Individual means for each of these measures were submitted to an ANOVA with RSVP structure (two-target vs. three-target) and Lag (3 vs. 9) as within-subject factors. The ANOVA confirmed that the P3b

amplitude was larger at lag 9 than at lag 3, $F(1, 39) = 27.6$, $\eta_p^2 = .411$, $p < .0001$, and larger in two-target than in three-target trials, $F(1, 39) = 9.0$, $\eta_p^2 = .192$, $p < .005$. Furthermore, Lag and RSVP structure interacted, with a larger attenuation of P3b amplitude in three-target trials relative to two-target trials at lag 3 than at lag 9, $F(1, 39) = 6.6$, $\eta_p^2 = .149$, $p < .02$. To characterize the interaction further, we compared the amplitude of the P3b across two-target and three-target trials in a separate ANOVA considering only trials at lag 9 and found no significant difference, $F < 1$, $p > .7$. At lag 3, in contrast, the amplitude of the P3b was larger in two-target trials than in three-target trials, $F(1, 39) = 14.1$, $\eta_p^2 = .266$, $p < .0006$.

Individual latency values of P3b responses to the last target in the streams (i.e., T3 in three-target trials or T2 in two-target trials) were submitted to an ANOVA using

Figure 2. Results of ERP analysis. Top graphs: Difference (target-present minus target-absent) ERP responses in two-target and three-target trials, plotted as a function of lag (3 vs. 9) observed at Pz (P3b) and Fz (P3a). Bottom scalp plots: Time course of voltage topographic scalp distribution in each of the four main conditions on the experimental design.
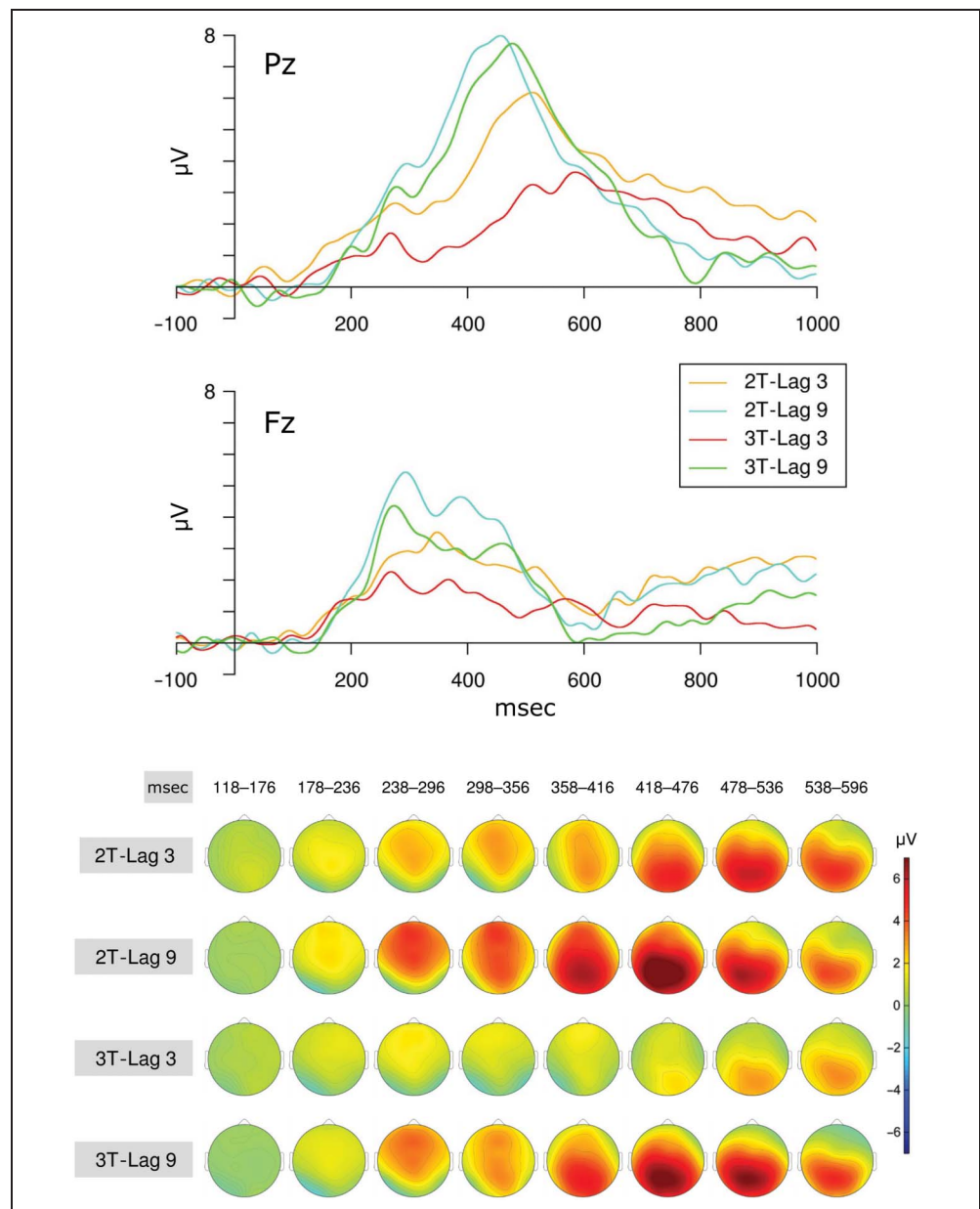
the same model as for the mean amplitudes analyses reported above. At lag 9, the mean latencies of the P3b response were 387 msec in two-target trials and 393 msec in three-target trials. At lag 3, the mean latencies of the P3b response were 434 msec in two-target trials and 483 msec in three-target trials. P3b latency was longer at lag 3 than at lag 9, $F(1, 39) = 38.7, \eta_p^2 = .199, p < .0001$, and longer in three-target trials than in two-target trials, $F(1, 39) = 9.4, \eta_p^2 = .567, p < .004$. Importantly, the difference in P3b latencies between two-target and three-target trials was larger at lag 3 than at lag 9, producing a significant interaction between RSVP structure and lag, $F(1, 39) = 4.5, \eta_p^2 = .102, p < .05$. We also compared two-target trials and three-target trials separately at each lag and observed no difference in P3b latencies between two-target trials and three-target trials at lag 9, $F(1, 39) = 1.6, p > .2$, but a clearly significant difference in P3b latencies between two-target trials and three-target trials at lag 3, $F(1, 39) = 8.7, \eta_p^2 = .189, p < .006$.

P3a

The main analyses were performed at Fz, at the peak of the scalp distribution of the P3a component. At lag 9, the mean amplitudes of the P3a response were 4.8 μV in two-target trials and 3.9 μV in three-target trials. At lag 3, the mean amplitudes of the P3a response were 2.9 μV in two-target trials and 1.9 μV in three-target trials. Individual means for each of these measures were submitted to an ANOVA with RSVP structure (two-target vs. three-target) and Lag (3 vs. 9) as within-subject factors. The ANOVA indicated a larger P3a amplitude at lag 9 than at lag 3, $F(1, 39) = 27.0, \eta_p^2 = .413, p < .0001$, and a larger P3a amplitude in two-target trials than in three-target trials, $F(1, 39) = 6.4, \eta_p^2 = .147, p < .02$. There was no interaction between RSVP structure and Lag in the analysis of P3a amplitude values recorded at Fz, $F < 1, p > .9$.

The mean P3a latency was 190 msec, and there were no significant differences across conditions in an ANOVA that considered RSVP structure and Lag as factors, all Fs < 1, all ps > .6, confirming what can be observed in Figure 2, namely, that, contrary to P3b, P3a latency was not subject to AB-induced perturbations.

ICA of ERPs

To further explore the interaction of detection and encoding processes in the AB, we performed ICA to decompose the ERPs into separate components using the algorithm implemented in EEGLAB (Delorme & Makeig, 2004). This was done to provide a more faithful depiction of the ERP results by decomposing P3a and P3b waveforms into maximally spatiotemporally independent signals available in the channel data and minimize to nil the influence of their potential overlap/summation on the interpretation of the above findings. The difference waves for the four main

conditions in the experiment (two-target vs. three-target trials × lag 3 vs. lag 9) for each participant were first analyzed using singular value decomposition to determine the dimensionality of the signal subspace containing most of the relevant event-related activity. A scree plot of the singular values showed a clear break after the first three components, leading us to retain the first four dimensions, which accounted for 54.3% of the variance. The ICA analysis was thus restricted to this subspace of the signal space using an initial PCA. The ICA analysis isolated two components of the P3 family, namely, a later posterior component (Component I, P3b) and an earlier anterior component (Component II, P3a). The grand-averaged time courses and relative topographies for these two components, for the four main conditions of the present experimental design, are shown in Figure 3. We reconstructed the time course for the two components of interest in the ICA analysis for each participant and condition and submitted amplitude and latency measures to the same type of ANOVA models as were used for the analyses of the original ERPs.

ICA-P3b

At lag 9, the mean amplitudes of the ICA-P3b were 4.1 μV in two-target trials and 3.94 μV in three-target trials. At lag 3, the mean amplitudes of the ICA-P3b were 3.1 μV in two-target trials and 1.7 μV in three-target trials. ICA-P3b amplitude was larger at lag 9 than at lag 3, $F(1, 39) = 32.9, \eta_p^2 = .466, p < .0001$. Furthermore, ICA-P3b amplitude was larger in two-target trials than in the three-target trials, $F(1, 39) = 13.7, \eta_p^2 = .269, p < .0001$. The difference between two-target and three-target trials was larger at lag 3 than at lag 9, which produced a significant interaction between RSVP structure and Lag, $F(1, 39) = 7.9, \eta_p^2 = .174, p < .008$. We also compared two-target and three-target trials separately at each lag. At lag 9, ICA-P3b amplitudes for two-target and three-target trials were equivalent, $F < 1, p > .7$. In contrast, at lag 3, ICA-P3b amplitudes for two-target and three-target trials differed substantially, $F(1, 39) = 14.1, \eta_p^2 = .264, p < .0006$.

At lag 9, the estimated mean ICA-P3b latencies were 390 msec for two-target trials and 396 msec for three-target trials. At lag 3, ICA-P3b latencies were 436 msec for two-target trials and 480 msec for three-target trials. This pattern of latencies produced a significant effect of Lag, $F(1, 39) = 57.65, \eta_p^2 = .674, p < .0001$, reflecting the general earlier latency of ICA-P3b components of two-target and three-target trials at lag 9 relative to lag 3. ICA-P3b latency was prolonged in three-target trials relative to two-target trials, $F(1, 39) = 16.0, \eta_p^2 = .295, p < .0003$, the more so at lag 3 compared with lag 9, $F(1, 39) = 5.7, \eta_p^2 = .138, p < .03$. We also compared two-target and three-target trials separately at each lag. At lag 9, ICA-P3b latencies for two-target and three-target trials were equivalent, $F(1, 39) = 2.5, p > .12$. In contrast, at lag 3, ICA-P3b

Figure 3. Results of ICA.
Top graphs: ERP functions
corresponding to ICA-P3b and
ICA-P3a isolated using ICA.
Bottom scalp plots: Scalp
topographic maps of ICA-P3b
(left) and ICA-P3a (right).
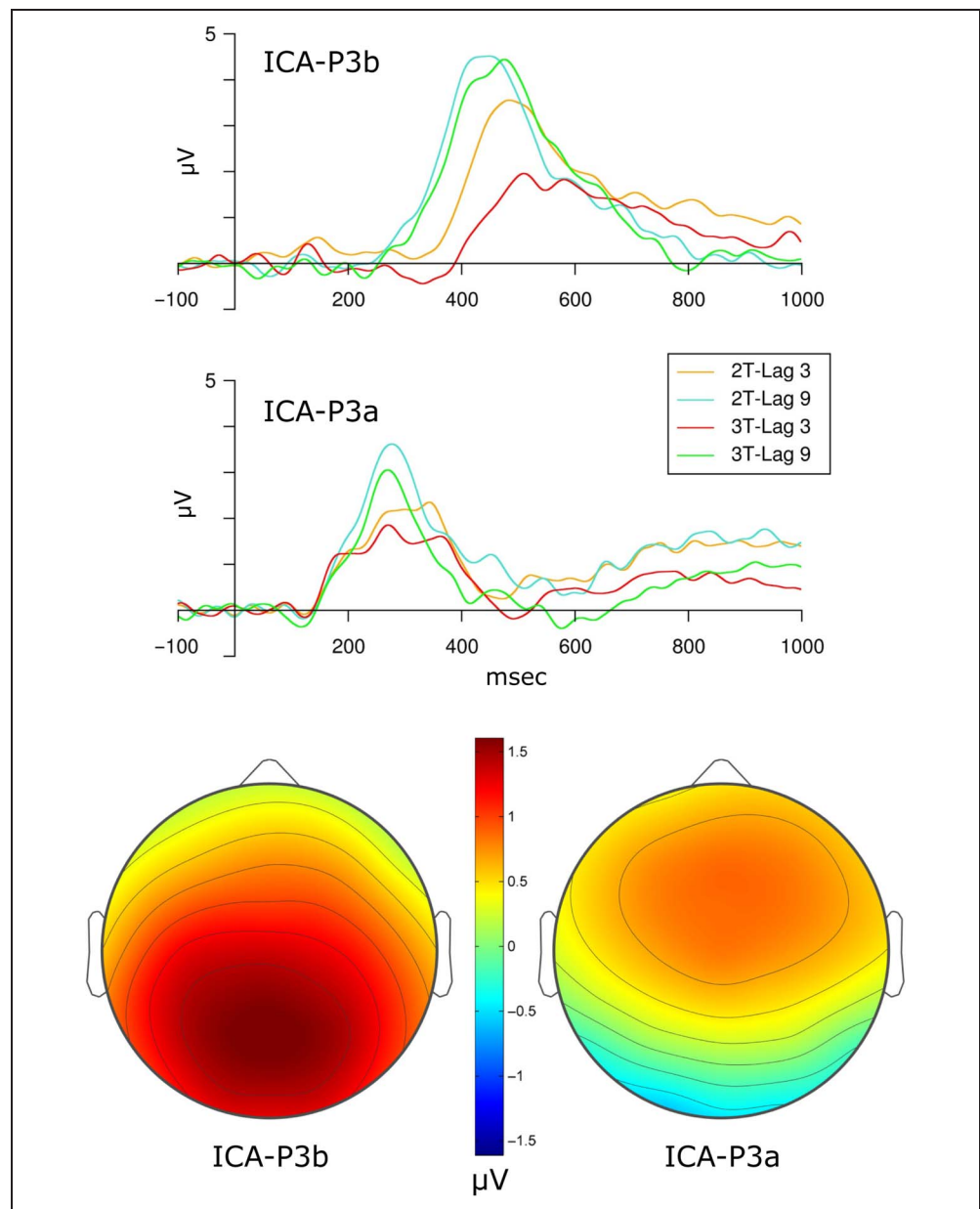
latencies for two-target and three-target trials differed substantially, $F(1, 39) = 13.9$, $\eta_p^2 = .264$, $p < .0007$.

ICA-P3a

At lag 9, the mean amplitudes of the ICA-P3a were 2.13 μV in two-target trials and 1.86 μV in three-target trials. At lag 3, the mean amplitudes of the ICA-P3a were 2.26 μV in two-target trials and 1.65 μV in three-target trials. ICA-P3a amplitude did not significantly differ between lags 3 and 9, $F(1, 39) = 1.9$, $p > .12$. ICA-P3a amplitude was however larger in two-target trials than in three-target trials, $F(1, 39) = 6.4$, $\eta_p^2 = .149$, $p < .02$. The difference between two-target and three-target waveforms was smaller at lag 9 than at lag 3, which produced a significant interaction between RSVP structure and Lag, $F(1, 39) = 3.7$, $\eta_p^2 = .128$, $p < .05$. Separate analyses confirmed that

ICA-P3a amplitude did not differ between two-target and three-target trials at lag 9, $F(1, 39) = 1.4$, $p < .3$, whereas this difference was significant at lag 3, $F(1, 39) = 6.7$, $\eta_p^2 = .185$, $p < .02$.

The mean latency of ICA-P3a was 175 msec. There were no significant differences across conditions, $F < 1$, $p > .8$, for both main effects and for the interaction. To further ascertain the absence of any latency effects on P3a, we also computed the offset latency of the ICA-P3a as the mean time-point when the descending portion of individual ICA-P3a waveforms crossed the 75% amplitude value. In both two-target and three-target trials, the mean ICA-P3a offset latencies were 331 msec at lag 9 and 383 msec at lag 3, reflected in a main effect of Lag, $F(1, 39) = 22.9$, $\eta_p^2 = .375$, $p < .0001$. However, as shown in Figure 3, the mean ICA-P3a offset latencies observed in two-target and three-target trials did not differ significantly, $F < 1$,

$p > .6$, nor was an interaction between RSVP structure and Lag observed, $F < 1, p > .6$.

Regression of ICA Components

A direct link between T3-locked ICA-P3a amplitude and offset and ICA-P3b latency was explored through multiple linear mixed-effect regression analyses carried out on 160 ICA-P3b values—40 participants, each contributing one value in four cells of the RSVP structure by lag design—analyzed in the foregoing sections.[1] The choice of both amplitude and offset to quantify ICA-P3a variations was based on the result of a preliminary analysis that revealed a positive correlation ($r = .28; p < .05$) between these two parameters across participants, as though greater P3a amplitude values were interindividually associated with slightly postponed P3a offset values.

A first regression explored the presence of a possible latent covariation between ICA-P3a and ICA-P3b parameters that were independent on the experimental variables manipulated in our design. The regression considered T3-locked ICA-P3b latency as dependent variable (y), T3-locked ICA-P3a amplitude (x1), and ICA-P3a offset (x2) as independent variables. The resulting linear model was:

$$y = 313 - 12.8_{(x1)} + 0.4_{(x2)} \qquad (1)$$

with a $R^2 = .55$, $t_{(x1)} = -4.6$, and $t_{(x2)} = 5.8$.

Model (1) was compared with the result of a second regression that was carried out on the same data set in which the four levels of the RSVP structure by lag design were explicitly included as independent factors, setting the least attention-demanding condition (i.e., two-target trials at lag 9; 2T-lag 9) as the baseline for contrasts against each of the other three conditions, that is, two-target trials at lag 3 (2T-lag 3) and three-target trials at
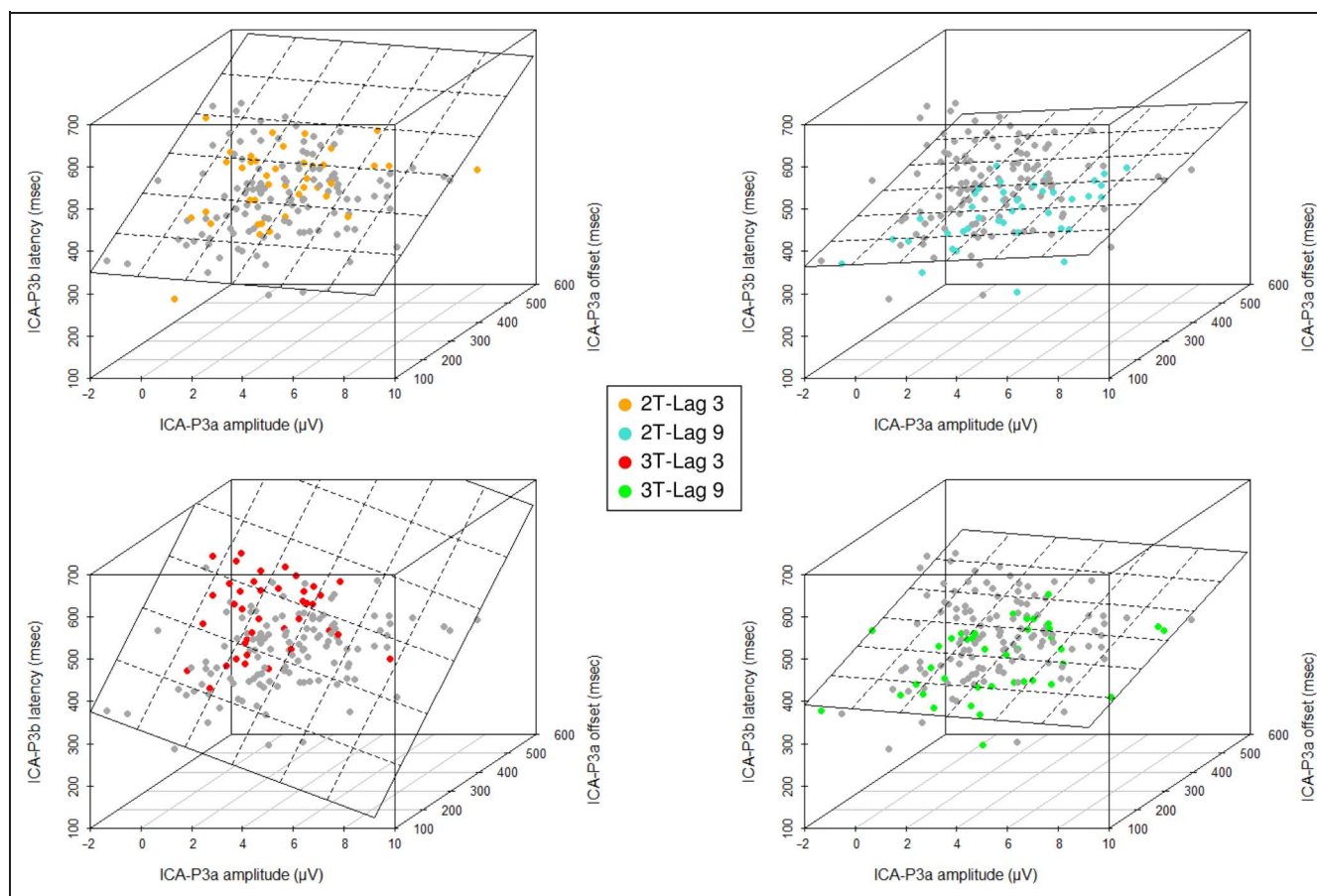

Figure 4. Results of the regressions on ICA-P3b latency values. ICA-P3b latency values in each scatterplot are reported as a function of the two predictors included in the regression models, ICA-P3a amplitude and ICA-P3a offset. Each scatterplot includes the entire data set of 160 ICA-P3b latency values—40 participants, each providing four ICA-P3b values in the RSVP structure (two-target vs. three-target trials) by lag (3 vs. 9) design—with the different conditions indicated by the different colors reported in the legend. All remnant gray dots in any given scatterplot correspond to ICA-P3b latency values in all the other three conditions. The plane intersecting the 3-D matrices in each scatterplot is a graphical representation of the linear model tested in each regression. Effects due to experimental manipulations are evident in the form of progressively increasing adherence of ICA-P3b latency values to the respective model (intersecting plane) from the least (2T-lag 9) to the most attention-demanding conditions (3T-lag 3).

lags 3 and 9 (3T-lag 3 and 3T-lag 9, respectively). The resulting linear model was:

$$y = 335 - 4.3_{(x1)} + 0.2_{(x2)} + 37.9_{(2T\text{-lag }3)}$$
$$+ 10.8_{(3T\text{-lag }9)} + 79.0_{(3T\text{-lag }3)} \tag{2}$$

with a $R^2 = .71$, $t_{(x1)} = -1.5$, $t_{(x2)} = 2.7$, $t_{(2T\text{-lag }3)} = 3.2$, $t_{(3T\text{-lag }9)} = 1.0$, and $t_{(3T\text{-lag }3)} = 6.3$.

Models (1) and (2) were submitted to a likelihood ratio test that indicated a Bayesian information criterion for the model (2) that was significantly smaller than the corresponding Bayesian information criterion for model (1) (1781 vs. 1803; $\chi^2(3) = 38.1$, $p < .0001$). The ratio between Bayes factors (Bf) corresponding to model (2) and model (1) was greater than 100, indicating that model (2) explained the relationship between ICA-P3a modulations and ICA-P3b latency shifts of several order of magnitude more precisely than model (1) (Kass & Raftery, 1995).

Separate linear regressions were carried out on the data from each cell of the RSVP structure by lag design to better qualify the effect of the experimental manipulations on the distribution of P3b latency values, which are graphed in Figure 4.

At lag 9, in both two-target (cyan) and three-target (green) trials, the respective linear models—visually represented in each panel by the plane intersecting the 3-D distribution of ICA-P3b latency values—were not significant (both $Fs < 1$, $ps > .5$). At lag 3, in contrast, the regression analysis on ICA-P3b latency values in two-target (yellow) trials considering T3-locked ICA-P3a amplitude and ICA-P3a offset as predictors indicated a significant impact of ICA-P3a amplitude (45.01, $t(38) = 1.64$, $p < .01$) and P3a offset (0.74, $t(38) = 3.19$, $p < .003$) and a marginally significant trend toward an interaction between ICA-P3a offset and amplitude (-0.12, $t(38) = -1.83$, $p < .07$), with a $R^2 = .23$, $F(3, 36) = 6.6$, $p < .03$. The regression analysis on ICA-P3b latency values in three-target (red) trials considering the same predictors indicated a significant impact of ICA-P3a amplitude (114.0, $t(38) = 1.93$, $p < .05$) and P3a offset (1.33, $t(38) = 3.75$, $p < .001$) and a significant interaction between ICA-P3a offset and amplitude (-0.34, $t(38) = -2.16$, $p < .04$), with a $R^2 = .35$, $F(3, 36) = 6.6$, $p < .03$. Note that R^2 values associated with each regression provide an estimate of the adherence of the cluster of ICA-P3b latency values in each experimental condition to the plane representing the tested model. As Figure 4 makes particularly clear, the adherence of ICA-P3b latency values increased from lag 9 to lag 3, the more so in three-target trials relative to two-target trials, as suggested by the increased R^2 parameters and ts associated with the interaction between ICA-P3a offset and amplitude.

DISCUSSION

To characterize how distinct information processing stages interact during the selection and encoding of visual infor-

mation distributed across time, we used an RSVP paradigm and manipulated the number of consecutive initial targets to modulate the magnitude of the AB (Dux et al., 2014). The last target in the RSVP streams was unmasked to allow the temporal dynamics of AB interference in the EEG signal to be observed in the absence of confounds from differing levels of accuracy on the final target (e.g., Ptito et al., 2008; Sessa et al., 2007; Vogel & Luck, 2002). Behaviorally, presenting two targets before the final target (three-target trials) reduced accuracy of the final target, although it was unmasked. This finding is generally more compatible with proposals that the AB is a target-induced phenomenon (Dux et al., 2014; Wyble et al., 2009, 2011; Dell'Acqua, Jolicœur, Luria, & Pluchino, 2009; Nieuwenstein, Potter, & Theeuwes, 2009; Dell'Acqua, Jolicœur, Pascali, & Pluchino, 2007; Visser, 2007) rather than a form of attentional perturbation induced by distractors (e.g., Taatgen, Juvina, Schipper, Borst, & Martens, 2009; Olivers & Meeter, 2008; Di Lollo, Kawahara, Ghorashi, & Enns, 2005; Raymond et al., 1992).

The electrophysiological measures showed clear anterior P3a and posterior P3b responses to the last target in the RSVP streams, and these were modulated differentially both by lag (3 vs. 9) and the number of preceding targets (1 vs. 2). The absolute magnitude of both ERP components was attenuated at short relative to long lags. However, there were key differences in these reductions with regards to latency and amplitude. Specifically, the P3a was reduced in amplitude, but its latency was unaffected by our manipulations. Conversely, the P3b exhibited both a decrease in amplitude and an increase in latency at short relative to long lags. Of import, this P3b latency increase for three- relative to two-target trials at the shorter lag could hardly be because of increased variance in the termination of pretarget(s) processing reflected in P3b jitter at short relative to long lags. In fact, Figure 2 reveals consistently higher amplitude values in the two-target relative to the three-target trials at lag 3 in the descending portion of P3b (compare orange and red functions in both graphs) suggesting—paradoxically—that more jitter was affecting two-target trials relative to three-target trials. This pattern was still present after isolating, via ICA analyses, the two components and fractionating the possible spatiotemporal overlap of P3a and P3b responses to the last target. Critically, the ICA reconstruction of P3b (Figure 3), at the shorter lag, shows a clear tendency of the P3b response in three-target trials to onset almost 100 msec after the P3b response in two-target trials. This strongly suggests that P3b component jitter is unlikely to be the cause of latency postponement affecting P3b responses elicited by the last target in two-target versus three-target trials. Rather, this finding complements and extends prior proposals referring to P3b as a signature of postponed consolidation of last target in working memory for delayed report by tying P3b amplitude and latency modulations to effects induced by the number of targets preceding the last target in RSVP sequences.

Crucially, P3a responses consistently preceded P3b responses, and this has been hypothesized to reflect the direction and/or temporal order of activation of the neural structures composing a frontotemporoparietal circuit enabling conscious vision of attended objects (Debener, Makeig, Delorme, & Engel, 2005; Daffner et al., 2003; Polich, 2003; Friedman et al., 2001; Gazzaniga et al., 2000; Soltani & Knight, 2000). The results of the regression analyses revealed a parametric link between P3a amplitude and P3b latency. At the longer lag, processing reflected in P3a responses was largely independent of processing occurring later and reflected by P3b responses, as shown by the absence of correlation between these estimates. At the shorter lag, in contrast, the amplitude of P3a responses was correlated with P3b response latency, suggesting that the observed delay in processing of the target within posterior brain areas results from reduced efficacy (i.e., amplitude) of the frontally mediated detection process. In this vein, we propose that P3a and P3b responses recorded during the AB are separate but interacting manifestations of two functional stages of processing involved in targets' conscious access: reduced efficacy of attentional recruitment in frontal areas (P3a) and a consequent delay in the processing of the target by posterior areas (P3b). These results corroborate current thinking about the crucial role of the frontal lobe in the control of selective attention and the establishment of conscious representations during perception (e.g., Cohen, Cavanagh, Chun, & Nakayama, 2012; Dell'Acqua et al., 2006; Corbetta, 1998; Desimone & Duncan, 1995). In addition, the present findings complement fMRI results by providing an electrophysiological signature recorded at scalp of the involvement of frontal structures in the AB effect (Kranczioch et al., 2005; Marois et al., 2004). We argue that this indexes the activation of a representational medium supplying visual information for working memory encoding/consolidation (Jolicœur & Dell'Acqua, 1998; or tokenization, Wyble et al., 2009). To note, the parietal negativity typically observed during working memory maintenance, termed contralateral delay activity (e.g., Vogel & Machizawa, 2004) or sustained posterior contralateral negativity (e.g., Luria, Sessa, Gotler, Jolicœur, & Dell'Acqua, 2010), which largely overlaps with P3b activity time window, has never been shown to be accompanied (or preceded) by frontal activity modulations. Frontal activity during working memory maintenance, however, has been detected intracranially in macaques by measuring local field potentials in frontal and supplementary eye field regions, whose activation is negatively correlated with power of oscillatory activity in the alpha range (8–13 Hz) in inferoparietal regions (Reinhart et al., 2012). In our view, this suggests a fundamental distinction between frontal activity (P3a) likely arising from an extended portion of the dorsolateral prefrontal cortex and subserving visual working memory encoding/consolidation and frontal activity subserving visual working memory maintenance, which appears to not be detectable at the scalp in humans but intracranially in specific and highly localized regions

(i.e., frontal and supplementary eye fields) of the macacque cortex.

Compared with the impressive corpus of studies focusing on the centroparietal P3b subcomponent of the P3 complex, the frontocentral P3a subcomponent has been the object of less investigation, and its functional connotation is still a matter of debate. The last decade of studies on P3a has unveiled a surprisingly tight connection between P3a and mental operations involved in attentional control. Indeed, contrary to the original depiction of P3a as a typical response to infrequent, novel, and contextually deviant stimuli (e.g., Friedman et al., 2001), more recent studies have provided evidence of P3a responses to task-relevant information displayed in a variety of cognitive tasks, like feedback signals displayed at the end of trials (e.g., Butterfield & Mangels, 2003), no-go signals in standard go/no-go designs (e.g., Rushworth, Walton, Kennerley, & Bannerman, 2004), and task-relevant stimuli displayed on first trials (e.g., Huettel, Mack, & McCarthy, 2002). In an elegant attempt at providing a unitary functional account of P3a activity encompassing these diverse experimental contexts, Barceló and colleagues (Barceló et al., 2006; Barceló, Periáñez, & Knight, 2002) devised a variant of a task-switch design in which one of four cards of the WCST had to be matched with a target card of the same set according to two alternating criteria, either on the basis of the color of the symbols on the cards or on the basis of the symbols' number. On any given trials, the criterion for the classification task was specified by a tonal cue before the onset of the target card, which indicated if the classification scheme had to be maintained for the incoming stimulus (repeat-cue) or changed (switch-cue). Randomly on a proportion of trials, a contextually deviant sound—always novel on each trial—was displayed during the interval between a repeat-cue and the target card. Interestingly, P3a responses of equal amplitude were detected in response to both deviant sounds and switch-cues, a finding strongly suggesting that a primary determinant of P3a activity in task-switch designs is attentional control demanded to (re)configure the mental set to carry out the classification task appropriately. Further work led these authors to put forth the hypothesis that the bursts of delta power, held to give rise to P3a responses, reflect inhibition of the current mental set to establish a different mental set (Prada, Barceló, Herrmann, & Escera, 2014).

This hypothesis is corroborated by studies on the AB that have shown a correlation between P3a amplitude and the probability of reporting T2 correctly in designs in which a task-switch was required to process T1 and T2. Sergent, Baillet, and Dehaene (2005; see also Marti, Sigman, & Dehaene, 2012) asked participants to distinguish between "XOOX/OXXO" strings displayed as T1 and to identify a T2 number word whose onset was signaled by four surrounding dots. P3a activity was detected for correctly reported T2 stimuli but not for missed items, as though the cause of the failure to report T2 could be ascribed to a failure to switch mental set or selection

criteria between the different tasks. Task-switching in RSVP designs is known to exacerbate AB effects (Kawahara, Zuvic, Enns, & Di Lollo, 2003), and this may be so because task-switching is controlled by frontal areas partly overlapping with those underpinning the deployment of top–down attention to target information (e.g., Cutini et al., 2008; Dove, Pollmann, Schubert, Wiggins, & von Cramon, 2000). However, task-switching between T1 and T2 processing in the AB has been hypothesized to draw on distinct capacity limitations relative to those held to constitute the root cause of the AB (Dale, Dux, & Arnell, 2013; Kelly & Dux, 2011; see Visser, Bischof, & Di Lollo, 1999, for a review).

One may still argue that P3a responses detected in the present experiment reflect some form of attention control processes directed at visual input, as proposed by Barceló and colleagues. These researchers suggests that task-switching is inextricably linked with multitarget RSVP designs where selection criterion and task requirements on targets are uniform (i.e., report letters embedded among digits). Targets in this case must undergo a set of mental operations optimized for successful classification whereas a different set of mental operations may be hypothesized to be required to inhibit distractors (e.g., Taatgen et al., 2009; Olivers & Meeter, 2008; Di Lollo et al., 2005). One critical finding that is at odds with this proposal, however, is that that P3a responses described by Barceló's and colleagues, though correlated with behavioral switch costs (Monsell, 2003), were not correlated with trailing target-locked P3b activity, contrary to what was observed here at the shorter intertarget lag.

Perhaps, a better functional connotation of P3a and P3b responses in the present context can be attempted by resorting to psychological theory, whereby the present electrophysiological results appear to corroborate AB models ascribing the phenomenon to inhibition of top–down attention to visual input. Wyble et al. (2011) have proposed that the AB reflects mechanisms involved in parsing the visual continuum into discrete visual episodes and memory representations and provided P3b evidence compatible with this idea (Craston, Wyble, Chennu, & Bowman, 2009). More specifically, the model put forward by Wyble et al. (2009) hinges on the principle that top–down attention allocation to preattentive target sensory representations— or target types—is instrumental to bring activation of these representations suprathreshold. This triggers in turn an encoding mechanism that binds target types to time-coding memory units denoting targets' episodic arrangement-producing target tokens. These tokens are maintained in visual working memory and are available for subsequent conscious report. While target encoding is under way (e.g., for T1 in standard two-target RSVP streams), top–down attention is momentarily inhibited so as to segregate T1 from trailing visual inputs (i.e., T2 or distractors) lagging T1 for longer than 200 msec. This processing dynamic is held to be at the root of the AB effect (and of the so-called lag 1 or protracted sparing effect; Dell'Acqua et al., 2012).

This model fits naturally in the present electrophysiological picture by assuming that P3a amplitude is a measure of top–down attention allocation efficiency and that P3b amplitude and latency are a combined estimate of working memory encoding processes. In this augmented framework, encoding two previous targets in three-target trials versus one previous target in two-target trials would take up more processing capacity and produce stronger inhibition of top–down attention allocation to the last target. This is captured in the present results by the amplitude attenuation of P3a response to the last target observed at short lag, which was more pronounced in three-target trials than in two-target trials. Furthermore, inhibited top–down attention to target types during the AB would delay encoding of the last target in the RSVP sequence at short relative to long lags. This increased delay would be reflected in the prolonged latency and sizable amplitude reduction of P3b observed at the short lag, which was more evident in three-target trials relative to two-target trials.

When describing their results with reference to P3b suppression during the AB, Vogel et al. (1998) reported a frontal positive ERP component that preceded temporally the posterior P3b, which they labeled P2. The P2 component showed amplitude suppression under the same AB conditions as those associated with P3b suppression, raising thus the possibility that the P2 and the present P3a may be manifestations of the same underlying mechanism. Despite similarities however, the P2 is primarily reactive when attentional selection occurs based on simple features (Luck & Hillyard, 1994), whereas P3a is a multimodal component elicited by a wide variety of stimuli. Indeed, the P2 found by Vogel et al. was observed under conditions where T2 had to be selected based on color (i.e., T2 was a white stimulus embedded among black distractors). Similarly, a T2-elicited P2 component has been reported by Pesciarelli et al. (2007), who used to-be-detected red targets interspersed among white distractors. These researchers explored the T2-locked P2 as a function of whether T2 was missed or correctly reported at short lags and found no P2 amplitude/latency difference between these two conditions. Pesciarelli concluded, contrary to Vogel et al. (1998), that the visual P2 was not influenced by the AB. P2 and P3a differ in this respect, because P3a is demonstrably evident following a correctly reported target and absent following a missed target (Sergent et al., 2005). Most importantly, P2 amplitude tends to increase with stimulus repetition, whereas P3a amplitude behaves in the opposite manner, increasing when stimuli are novel and/or infrequent (Curran & Dien, 2003; Misra & Holcombe, 2003; Rugg, 1987). Collectively, these empirical observations reinforce our conclusions that the frontal subcomponent of the P3 complex evident in this study was really a P3a ERP component and not a P2.

To summarize, using a multitarget RSVP design and manipulating intertarget lag, we replicated and extended prior findings indicating reduced amplitude and latency postponement of last target-locked P3b activity at short

relative to long lags. This AB effect on P3b was dependent on target load, as these modulations were more pronounced in three-target trials, in which the last target was preceded by two to-be-encoded targets, than in two-target trials, in which the last target was preceded by just one to-be encoded item. An important and novel result was the clear AB effect on P3a responses, which were analogous in terms of amplitude modulations to P3b, but different in terms of latency, as no postponement was observed on the onset of this component. We have proposed that Wyble's et al. (2011) computational account of the AB offers a unitary framework where all of the present results can be interpreted collectively. We propose that suppression of P3a amplitude can be taken as evidence of reduced attention allocation efficiency for detecting the last target during the AB window, which in turn leads to a prolongation of the time taken to stabilize the sensory trace for generation of the conscious visual episode enabling delayed report of the last target.

Acknowledgments

Note

1.   We opted for mixed-effect regressions that considered participants as random factor to circumvent the violation of independence due to the fact that each participant contributed four (2 RSVP structures by 2 lags) nonindependent P3b latency values to the final data set. Relative to standard null-hypothesis statistical testing, the probability distributions of statistical parameters generated using the present approach are not known a priori, which makes reporting p values uninformative (see Baayen, Davidson, & Bates, 2008, for details). R^2 in mixed-effect regressions was approximated using the algorithm proposed by Xu (2003).

REFERENCES

Akyürek, E. G., Leszczyński, M., & Schubö, A. (2010). The temporal locus of the interaction between working memory consolidation and the attentional blink. *Psychophysiology, 47,* 1134–1141.

Baars, B. (1989). *A cognitive theory of consciousness.* New York: Cambridge University Press.

Baayen, R. H., Davidson, D. J., & Bates, D. M. (2008). Mixed-effects modeling with crossed random effects for subjects and items. *Journal of Memory and Language, 59,* 390–412.

Barceló, F., Escera, C., Corral, M. J., & Periáñez, J. A. (2006). Task switching and novelty processing activate a common neural network for cognitive control. *Journal of Cognitive Neuroscience, 18,* 1734–1748.

Barceló, F., Periáñez, J. A., & Knight, R. T. (2002). Think differently: A brain orienting response to task novelty. *NeuroReport, 13,* 1887–1892.

Bastiaansen, M., Mazaheri, A., & Jensen, O. (2012). Beyond ERPs: Oscillatory neuronal dynamics. In S. J. Luck & E. S. Kappenman (Eds.), *The Oxford handbook of event-related potential components* (pp. 31–49). New York: Oxford University Press.

Batterink, L., Karns, C. M., Yamada, Y., & Neville, H. (2010). The role of awareness in semantic and syntactic processing: An ERP attentional blink study. *Journal of Cognitive Neuroscience, 22,* 2514–2529.

Benjamini, Y., & Hochberg, Y. (1995). Controlling the false discovery rate: A practical and powerful approach to multiple testing. *Journal of the Royal Statistical Society, Series B, 57,* 289–300.

Bledowski, C., Prvulovic, D., Goebel, R., Zanella, F., & Linden, D. (2004). Attentional systems in target and distractor processing: A combined ERP and fMRI study. *Neuroimage, 22,* 530–540.

Bledowski, C., Prvulovic, D., Hoechstetter, K., Scherg, M., Wibral, M., Goebel, R., et al. (2004). Localizing P300 generators in visual target and distracter processing: A combined event-related potential and functional magnetic resonance imaging study. *Journal of Neuroscience, 24,* 9353–9360.

Brisson, B., & Bourassa, M. È. (2014). Masking of a first target in the attentional blink attenuates the P3 to the first target and delays the P3 to the second target. *Psychophysiology, 51,* 611–619.

Brisson, B., & Jolicœur, P. (2008). Express attentional re-engagement but delayed entry into consciousness following invalid spatial cues in visual search. *PLoS One, 3,* e3967.

Butterfield, B., & Mangels, J. A. (2003). Neural correlates of error detection and correction in a semantic retrieval task. *Cognitive Brain Research, 17,* 793–817.

Chennu, S., Craston, P., Wyble, B., & Bowman, H. (2009). Attention increases the temporal precision of conscious perception: Verifying the neural-ST^2 model. *PLoS Computational Biology, 5,* e1000576.

Choi, H., Chang, L. H., Shibata, K., Sasaki, Y., & Watanabe, T. (2012). Resetting capacity limitations revealed by long-lasting elimination of attentional blink through training. *Proceedings of the National Academy of Sciences, U.S.A., 109,* 12242–12247.

Chun, M. M., & Potter, M. C. (1995). A two-stage model for multiple target detection in rapid serial visual presentation. *Journal of Experimental Psychology: Human Perception and Performance, 21,* 109–127.

Cohen, M. A., Cavanagh, P., Chun, M. M., & Nakayama, K. (2012). The attentional requirements of consciousness. *Trends in Cognitive Sciences, 16,* 411–417.

Coltheart, M. (1980). Iconic memory and visible persistence. *Perception & Psychophysics, 27,* 183–228.

Colzato, L. S., Slagter, H. A., de Rover, M., & Hommel, B. (2011). Dopamine and the management of attentional resources: Genetic markers of striatal D2 dopamine predict individual differences in the attentional blink. *Journal of Cognitive Neuroscience, 23,* 3576–3585.

Corbetta, M. (1998). Frontoparietal cortical networks for directing attention and the eye to visual locations: Identical, independent, or overlapping neural systems? *Proceedings of the National Academy of Sciences, U.S.A., 95,* 831–838.

Corbetta, M., & Shulman, G. L. (2002). Control of goal-directed and stimulus-driven attention in the brain. *Nature Reviews Neuroscience, 3,* 201–215.

Courchesne, E., Hillyard, S. A., & Galambos, R. (1975). Stimulus novelty, task relevance, and the visual evoked potential in

man. *Electroencephalography and Clinical Neurophysiology, 39,* 3336–3338.

Craston, P., Wyble, B., Chennu, S., & Bowman, H. (2009). The attentional blink reveals serial working memory encoding: Evidence from virtual and human event-related potentials. *Journal of Cognitive Neuroscience, 21,* 550–566.

Curran, T., & Dien, J. (2003). Differentiating amodal familiarity from modality-specific memory processes: An ERP study. *Psychophysiology, 40,* 979–988.

Cutini, S., Scatturin, P., Menon, E., Bisiacchi, P., Gamberini, L., Zorzi, M., et al. (2008). Selective activation of the superior frontal gyrus in task-switching: An event-related fNIRS study. *Neuroimage, 42,* 945–955.

Cycowicz, Y. M., & Friedman, D. (1998). Effects of sound familiarity on the event-related potentials elicited by novel environmental sounds. *Brain and Cognition, 36,* 30–51.

Daffner, K. R., Scinto, L. F. M., Weitzman, A. M., Faust, R., Rentz, D. M., Budson, A. E., et al. (2003). Frontal and parietal components of a cerebral networks mediating voluntary attention to novel events. *Journal of Cognitive Neuroscience, 15,* 294–313.

Dale, G., Dux, P. E., & Arnell, K. A. (2013). Individual differences within and across attentional blink tasks revisited. *Attention, Perception, & Psychophysics, 75,* 456–467.

Debener, S., Makeig, S., Delorme, A., & Engel, A. K. (2005). What is novel in the novelty oddball paradigm? Functional significance of the novelty P3 event-related potential as revealed by independent component analysis. *Cognitive Brain Research, 22,* 309–321.

Dehaene, S., Sergent, C., & Changeux, J. P. (2003). A neuronal network model linking subjective experience and objective physiological data during conscious perception. *Proceedings of the National Academy of Sciences, U.S.A., 100,* 8520–8525.

Dell'Acqua, R., Dux, P. E., Wyble, B., & Jolicœur, P. (2012). Sparing from the attentional blink is not spared from structural limitations. *Psychonomic Bulletin & Review, 19,* 232–238.

Dell'Acqua, R., Jolicœur, P., Luria, R., & Pluchino, P. (2009). Reevaluating encoding-capacity limitations as a cause of the attentional blink. *Journal of Experimental Psychology: Human Perception and Performance, 35,* 338–351.

Dell'Acqua, R., Jolicœur, P., Pascali, A., & Pluchino, P. (2007). Short-term consolidation of individual identities leads to lag-1 sparing. *Journal of Experimental Psychology: Human Perception and Performance, 33,* 593.

Dell'Acqua, R., Sessa, P., Jolicœur, P., & Robitaille, N. (2006). Spatial attention freezes during the attention blink. *Psychophysiology, 43,* 394–400.

Delorme, A., & Makeig, S. (2004). EEGLAB: An open source toolbox for analysis of single-trial EEG dynamics including independent component analysis. *Journal of Neuroscience Methods, 134,* 9–21.

Desimone, R., & Duncan, J. (1995). Neural mechanisms of selective visual attention. *Annual Review of Neuroscience, 18,* 193–222.

Di Lollo, V., Enns, J. T., & Rensink, R. A. (2000). Competition for consciousness among visual events: The psychophysics of reentrant visual processes. *Journal of Experimental Psychology: General, 129,* 481–507.

Di Lollo, V., Kawahara, J., Ghorashi, S. M. S., & Enns, J. T. (2005). The attentional blink: Resource depletion of temporary loss of control? *Psychological Research, 69,* 191–200.

Dove, A., Pollmann, S., Schubert, T., Wiggins, C. J., & von Cramon, D. Y. (2000). Prefrontal cortex activation in task switching: An event-related fMRI study. *Cognitive Brain Research, 9,* 103–109.

Dux, P. E., & Marois, R. (2009). The attentional blink: A review of data and theory. *Attention, Perception, & Psychophysics, 71,* 1683–1700.

Dux, P. E., Wyble, B., Jolicœur, P., & Dell'Acqua, R. (2014). On the costs of lag-1 sparing. *Journal of Experimental Psychology: Human Perception and Performance, 40,* 416–428.

Fabiani, M., & Donchin, E. (1995). Encoding processes and memory organization: A model of the von Restorff effect. *Journal of Experimental Psychology: Learning, Memory and Cognition, 21,* 224–240.

Fahrenfort, J. J., Scholte, H. S., & Lamme, V. A. F. (2007). Masking disrupts reentrant processing in human visual cortex. *Journal of Cognitive Neuroscience, 19,* 1488–1497.

Friedman, D., Cycowicz, Y. M., & Gaeta, H. (2001). The novelty P3: An event-related brain potential (ERP) sign of the brain's evaluation of novelty. *Neuroscience and Biobehavioral Reviews, 25,* 355–373.

Gazzaniga, M., Ivry, R. B., & Mangun, G. R. (2000). *Cognitive neuroscience: The biology of the mind.* New York: Norton & Company Inc.

Giesbrecht, B., & Di Lollo, V. (1998). Beyond the attentional blink: Visual masking by object substitution. *Journal of Experimental Psychology: Human Perception and Performance, 24,* 1454–1466.

Gross, J., Schmitz, F., Schnitzler, I., Kessler, K., Shapiro, K., Hommel, B., et al. (2004). Modulation of long-range neural synchrony reflects temporal limitations of visual attention in humans. *Proceedings of the National Academy of Sciences, U.S.A., 101,* 13050–13055.

Hanslmayr, S., Gross, J., Klimesch, W., & Shapiro, K. L. (2011). The role of α oscillations in temporal attention. *Brain Research Reviews, 67,* 331–343.

Harris, J. A., McMahon, A. R., & Woldorff, M. G. (2013). Disruption of visual awareness during the attentional blink is reflected by selective disruption of late-stage neural processing. *Journal of Cognitive Neuroscience, 25,* 1863–1874.

Hommel, B., Kessler, K., Schmitz, F., Gross, J., Akyürek, E., Shapiro, K., et al. (2006). How the brain blinks: Towards a neurocognitive model of the attentional blink. *Psychological Research, 70,* 425–435.

Huettel, S. A., Mack, P. B., & McCarthy, G. (2002). Perceiving patterns in random series: Dynamic processing of sequence in prefrontal cortex. *Nature Neuroscience, 5,* 485–490.

Jannati, A., Spalek, T. M., & Di Lollo, V. (2011). Neither backward masking of T2 nor task switching is necessary for the attentional blink. *Psychonomic Bulletin & Review, 18,* 70–75.

Jannati, A., Spalek, T. M., Lagroix, H. E. P., & Di Lollo, V. (2012). The attentional blink is not affected by backward masking of T2, T2-mask SOA, or level of T2 impoverishment. *Journal of Experimental Psychology: Human Perception and Performance, 38,* 161–168.

Johnson, R. (1993). On the neural generators of the P300 component of the event-related potential. *Psychophysiology, 30,* 90–97.

Johnson, R. (1995). Event-related potential insights into the neurobiology of memory systems. In F. Boller & J. Grafman (Eds.), *Handbook of neuropsychology* (pp. 135–163). Amsterdam: Elsevier.

Jolicœur, P., & Dell'Acqua, R. (1998). The demonstration of short-term consolidation. *Cognitive Psychology, 36,* 138–202.

Jung, T. P., Makeig, S., Humphries, C., Lee, T. W., McKeown, M. J., Iragui, V., et al. (2000). Removing electroencephalographic artifacts by blind source separation. *Psychophysiology, 37,* 163–178.

Kass, R. E., & Raftery, A. E. (1995). Bayes factors. *Journal of the American Statistical Association, 90,* 773–795.

Kawahara, J. I., Zuvic, S. M., Enns, J. T., & Di Lollo, V. (2003). Task switching mediates the attentional blink even without backward masking. *Perception & Psychophysics, 65,* 339–351.

Kelly, A. J., & Dux, P. E. (2011). Different attentional blink tasks reflect distinct information processing limitations: An individual differences approach. *Journal of Experimental Psychology: Human Perception and Performance, 37,* 1867–1873.

Kiesel, A., Miller, J., Jolicœur, P., & Brisson, B. (2008). Measurement of ERP latency differences: A comparison of single-participant and jackknife-based scoring methods. *Psychophysiology, 45,* 250–274.

Knight, R. T. (1991). Evoked potential studies of attention capacity in human frontal lobe lesions. In H. S. Levin, H. M. Eisenberg, & A. L. Benton (Eds.), *Frontal lobe function and dysfunction* (pp. 139–153). New York: Oxford University Press.

Koechlin, E., Ody, C., & Kouneiher, F. (2003). The architecture of cognitive control in the human prefrontal cortex. *Science, 302,* 1181–1185.

Kranczioch, C., Debener, S., & Engel, A. K. (2003). Event-related brain potential correlates of the attentional blink phenomenon. *Cognitive Brain Research, 17,* 177–187.

Kranczioch, C., Debener, S., Maye, A., & Engel, A. K. (2007). Temporal dynamics of access to consciousness in the attentional blink. *Neuroimage, 37,* 947–955.

Kranczioch, C., Debener, S., Schwarzbach, J., Goebel, R., & Engel, A. K. (2005). Neural correlates of conscious perception in the attentional blink. *Neuroimage, 24,* 704–714.

Lamme, V. A. F., & Roelfsema, P. R. (2000). The distinct modes of vision offered by feedforward and recurrent processing. *Trends in Neuroscience, 23,* 571–579.

Luck, S., & Hillyard, S. A. (1994). Electrophysiological correlates of feature analysis during visual search. *Psychophysiology, 31,* 291–308.

Luria, R., Sessa, P., Gotler, A., Jolicœur, P., & Dell'Acqua, R. (2010). Visual short-term memory capacity for simple and complex objects. *Journal of Cognitive Neuroscience, 22,* 496–512.

MacLean, M. H., & Arnell, K. M. (2011). Greater attentional blink magnitude is associated with higher levels of anticipatory attention as measured by alpha event-related desynchronization (ERD). *Brain Research, 1387,* 99–107.

Marcantoni, W. S., Lepage, M., Beaudoin, G., Bourgouin, P., & Richer, F. (2003). Neural correlates of dual task interference in rapid visual streams: An fMRI study. *Brain and Cognition, 53,* 318–321.

Marois, R., & Ivanoff, J. (2005). Capacity limits of information processing in the brain. *Trends in Cognitive Sciences, 9,* 296–305.

Marois, R., Yi, D. J., & Chun, M. M. (2004). The neural fate of consciously perceived and missed events in the attentional blink. *Neuron, 41,* 465–472.

Martens, S., & Wyble, B. (2010). The attentional blink: Past, present, and future of a blind spot in perceptual awareness. *Neuroscience and Biobehavioral Reviews, 34,* 947–957.

Marti, S., Sigman, M., & Dehaene, S. (2012). A shared cortical bottleneck underlying attentional blink and psychological refractory period. *Neuroimage, 59,* 2883–2898.

Misra, M., & Holcombe, P. J. (2003). Event-related potential indices of masked repetition priming. *Psychophysiology, 40,* 115–130.

Monsell, S. (2003). Task switching. *Trends in Cognitive Sciences, 7,* 134–140.

Nakatani, C., Ito, J., Nikolaev, A. R., Gong, P., & van Leeuwen, C. (2005). Phase synchronization analysis of EEG during attentional blink. *Journal of Cognitive Neuroscience, 17,* 1969–1979.

Nieuwenhuis, S., Gilzenrat, M. S., Holmes, B. D., & Cohen, J. D. (2005). The role of the locus coeruleus in mediating the attentional blink: A neurocomputational theory. *Journal of Experimental Psychology: General, 134,* 291–307.

Nieuwenstein, M. R., Potter, M. C., & Theeuwes, J. (2009). Unmasking the attentional blink. *Journal of Experimental Psychology: Human Perception and Performance, 35,* 159–169.

Olivers, C. N. L., & Meeter, M. (2008). A boost and bounce theory of temporal attention. *Psychological Review, 115,* 836–863.

Pesciarelli, F., Kutas, M., Dell'Acqua, R., Peressotti, F., Job, R., & Urbach, T. P. (2007). Semantic and repetition priming within the attentional blink: An event-related brain potential (ERP) investigation. *Biological Psychology, 76,* 21–30.

Polich, J. (2003). Overview of P3a and P3b. In J. Polich (Ed.), *Detection of change: Event-related potential and fMRI findings* (pp. 83–98). Boston, MA: Kluwer.

Polich, J. (2007). Updating P300: An integrative theory of P3a and P3b. *Clinical Neurophysiology, 118,* 2128–2148.

Polich, J., & Comerchero, M. D. (2003). P3a from visual stimuli: Typicality, task, and topography. *Brain Topography, 15,* 141–152.

Prada, L., Barceló, F., Herrmann, C. S., & Escera, C. (2014). EEG delta oscillations index inhibitory control of contextual novelty to both irrelevant distracters and relevant task-switch cues. *Psychophysiology, 51,* 658–672.

Ptito, A., Arnell, K. M., Jolicœur, P., & MacLeod, J. (2008). Intramodal and crossmodal processing delays in the attentional blink paradigm revealed by event-related potentials. *Psychophysiology, 45,* 794–803.

Raymond, J. E., Shapiro, K. L., & Arnell, K. M. (1992). Temporary suppression of visual processing in an RSVP task: An attentional blink? *Journal of Experimental Psychology: Human Perception and Performance, 18,* 849–860.

Reinhart, R. M. G., Heitz, R. P., Purcell, B. A., Weigand, P. K., Schall, J. D., & Woodman, G. F. (2012). Homologous mechanisms of visuospatial working memory maintenance in macaque and human: Properties and sources. *Journal of Neuroscience, 32,* 7711–7722.

Rugg, M. D. (1987). Dissociation of semantic priming, word and non-word repetition effects by event-related potentials. *Quarterly Journal of Experimental Psychology, 39,* 123–147.

Rushworth, M. F., Walton, M. E., Kennerley, S. W., & Bannerman, D. M. (2004). Action sets and decisions in the medial frontal cortex. *Trends in Cognitive Sciences, 8,* 410–417.

Scalf, P. E., Dux, P. E., & Marois, R. (2011). Working memory encoding delays top–down attention to visual cortex. *Journal of Cognitive Neuroscience, 23,* 2593–2604.

Sergent, C., Baillet, S., & Dehaene, S. (2005). Timing of the brain events underlying access to consciousness during the attentional blink. *Nature Neuroscience, 8,* 1391–1400.

Sessa, P., Luria, R., Verleger, R., & Dell'Acqua, R. (2007). P3 latency shifts in the attentional blink: Further evidence for second target processing postponement. *Brain Research, 1137,* 131–139.

Slagter, H. A., Tomer, R., Christian, B. T., Fox, A. S., Colzato, L. S., King, C. R., et al. (2012). PET evidence for a role of striatal dopamine in the attentional blink: Functional implications. *Journal of Cognitive Neuroscience, 24,* 1932–1940.

Smulders, F. T. Y. (2010). Simplifying jackknifing of ERPs and getting more out of it: Retrieving estimates of participants' latencies. *Psychophysiology, 47,* 387–392.

Soltani, M., & Knight, R. T. (2000). Neural origins of the P300. *Critical Reviews in Neurobiology, 14,* 199–224.

Taatgen, N. A., Juvina, I., Schipper, M., Borst, J. P., & Martens, S. (2009). Too much control can hurt: A threaded cognition model of the attentional blink. *Cognitive Psychology, 59,* 1–29.

Ulrich, R., & Miller, J. (2001). Using the jackknife-based scoring method for measuring LRP onset effects in factorial designs. *Psychophysiology, 38,* 816–827.

Visser, T. A. W. (2007). Masking T1 difficulty: Processing time and the attentional blink. *Journal of Experimental Psychology: Human Perception and Performance, 33,* 285–297.

Visser, T. A. W., Bischof, W. F., & Di Lollo, V. (1999). Attentional switching in spatial and nonspatial domains: Evidence from the attentional blink. *Psychological Bulletin, 125,* 458–469.

Vogel, E. K., & Luck, S. J. (2002). Delayed working memory consolidation during the attentional blink. *Psychonomic Bulletin & Review, 9,* 739–743.

Vogel, E. K., Luck, S. J., & Shapiro, K. L. (1998). Electrophysiological evidence for a postperceptual locus of suppression during the attentional blink. *Journal of Experimental Psychology: Human Perception and Performance, 24,* 1656–1674.

Vogel, E. K., & Machizawa, M. G. (2004). Neural activity predicts individual differences in visual working memory capacity. *Nature, 428,* 748–751.

Williams, M. A., Visser, T. A. W., Cunnington, R., & Mattingley, J. B. (2008). Attenuation of neural responses in primary visual cortex during the attentional blink. *Journal of Neuroscience, 28,* 9890–9894.

Wyble, B., Bowman, H., & Nieuwenstein, M. (2009). The attentional blink provides episodic distinctiveness: Sparing at a cost. *Journal of Experimental Psychology: Human Perception and Performance, 35,* 787–807.

Wyble, B., Potter, M. C., Bowman, H., & Nieuwenstein, M. (2011). Attentional episodes in visual perception. *Journal of Experimental Psychology: General, 140,* 488–505.

Xu, R. (2003). Measuring explained variation in linear mixed effects models. *Statistics in Medicine, 22,* 3527–3541.